Chapter 5

Instrumentation and Application Examples in Analytical Fourier Transform Mass Spectrometry

Frank H. Laukien [1], M. Allemann [2], P. Bischofberger [2], P. Grossmann [2], Hp. Kellerhals [2], and P. Kofel [2]

[1]Department of Chemical Physics, Harvard University, Cambridge, MA 02138

[2]Spectrospin AG, Industriestrasse 26, CH-8117 Fallanden, Switzerland

Selected topics in Fourier-Transform Ion Cyclotron Resonance Mass Spectrometry instrumentation are discussed in depth, and numerous analytical application examples are given. In particular, optimization ofthe single-cell FTMS design and some of its analytical applications, like pulsed-valve CI and CID, static SIMS, and ion clustering reactions are described. Magnet requirements and the software used in advanced FTICR mass spectrometers are considered. Implementation and advantages of an external differentially-pumped ion source for LD, GC/MS, liquid SIMS, FAB and LC/MS are discussed in detail, and an attempt is made to anticipate future developments in FTMS instrumentation.

It is not the intention of this chapter to provide a comprehensive treatment of FTMS technology and instrumentation, since excellent reviews exist (1). Instead, the focus will be on selected instrumental requirements which are crucial for the performance of a modern FTICR mass spectrometer, and which are not usually discussed elsewhere. Rather than striving for comprehensiveness, this paper is written with the intention of discussing specific design aspects in depth; the emphasis is on the unique features of our mass spectrometer, since other instrumental aspects are elaborated on elsewhere in this book.

Specifically, four instrumental topics are covered: First, our design criteria for an optimized single cell are explained and illustrated by several analytical application examples, including pulsed-valve CI and CID, static SIMS, and gas-phase polymerization reactions. Second, we explore the magnet requirements of FTMS as far as field strength, homogeneity and stability are concerned. Third, we offer our design philosophy for FTMS applications software, and the rationale for some unique features like phasing, the provisions for rapid scan/correlation ICR, timesharing, and versatile experimental event sequencing. Fourth, we discuss and illustrate

[1]Correspondence should be addressed to this author.

0097-6156/87/0359-0081$06.00/0

with analytical examples the desirability of a differentially-pumped ion source in general, and our implementation of external ionization in particular. Finally, an outlook on the anticipated future development of FTMS instrumentation and analytical techniques is provided.

Single-Cell FTMS: Design and Applications

ICR Cell Design. The exact geometry of the ICR cell is experimentally not critical, except possibly in ultra-high resolution measurements. The experimental fact that in terms of both resolution and mass accuracy, elongated rectangular, cylindrical, and Penning traps are more or less equivalent, has been corroborated theoretically (2). The choice of geometry is therefore determined by the desirability of maximizing the cell diameter and volume for a given magnet and vacuum system, while retaining good resolution and undistorted line-shapes. For the cylindrically symmetric environment near the magnetic center of a supercon magnet, a cylindrical cell, as depicted in Figure 1, maximizes the cell diameter d_x perpendicular to B. The volume of the cell employed in the CMS 47 is 170 ccm, and $d_x = d_z = 60$ mm.

If elongated cells ($d_z > d_x$) are utilized, we experimentally observe a degradation of both resolution and line-shape, presumably because the length of the homogeneous magnetic field region is approximately 60 mm.

The use of large cells in FTMS is advantageous, firstly because the volume of the quadrupolar electric field region is maximized and line-broadenings are therefore reduced, and secondly because the maximum trapping time increases with d_{x2}. This last point is particularly important if one is interested in large ion clusters which build up via gas-phase ion-neutral reactions. The average number of ion-neutral collisions C (and hence the maximum cluster size) which can occur before the ion clusters are lost at the side walls is proportional to the square of the product of magnetic field strength B and cell diameter d_x according to (3)

$$C \propto (d_x B)^2 / V \qquad (1).$$

Here V is the trapping voltage; note that C is pressure-independent.

An example of large negative ion clusters building up from smaller parent ions in the ICR cell is given in Figure 2a, where the Re_{17}^- and Re_{18}^--groups are selected from the negative ion-cluster mass spectrum of decacarbonyldirhenium. After electron capture and loss of one or several carbonyl groups, negative rheniumcarbonyl clusters polymerize up to $Re^1{}_8(CO)_{31}^-$ at mass M = 4,216 amu; they can still be observed with unit resolution. Positive rheniumcarbonyl clusters up to M = 8,828 amu are plotted in Figure 2b. The average number of collisions experienced by the parent ion of mass 652 amu is approximately C = 15,000. The average collision number for smaller ions, such as water, can be as high as 400,000.

All broadband spectra were amplified by a low-noise preamplifier with a dynamic range > 1,000, and a broadband main amplifier. The amplified time-domain signal is digitized by a 20 MHz, 9 bit Bruker ADC with 128 K words of buffer memory, and Fourier transformed by a Bruker array processor (128 K word FFT in 8 sec).

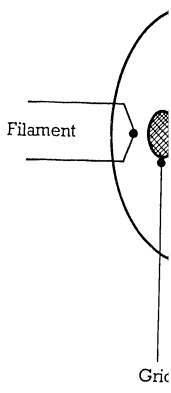

Figure 1. Cylinc
indicated are sui
for the study of

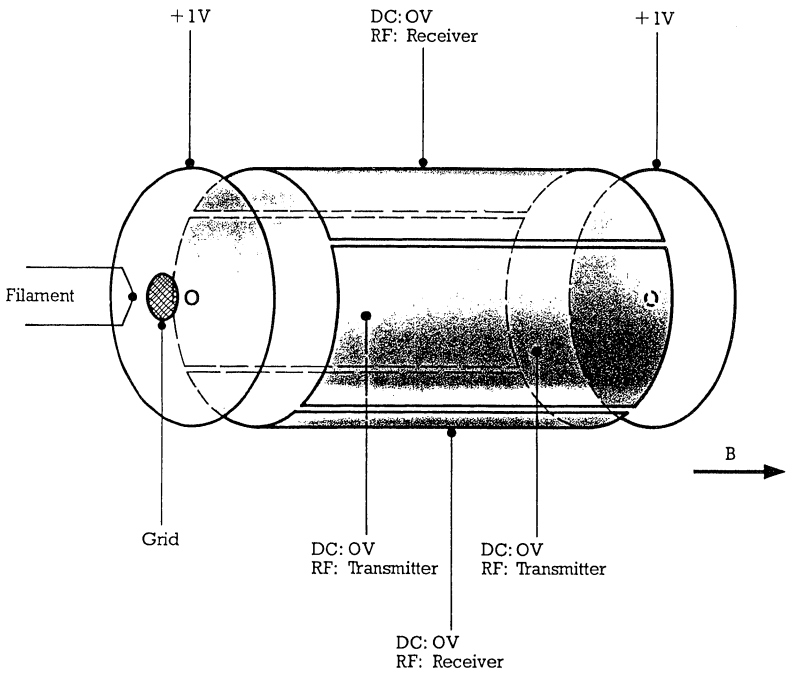

Figure 1. Cylindrical ICR cell with $d_x = d_z = 60$mm. The voltages indicated are suitable for positive ions and can simply be reversed for the study of negative ions.

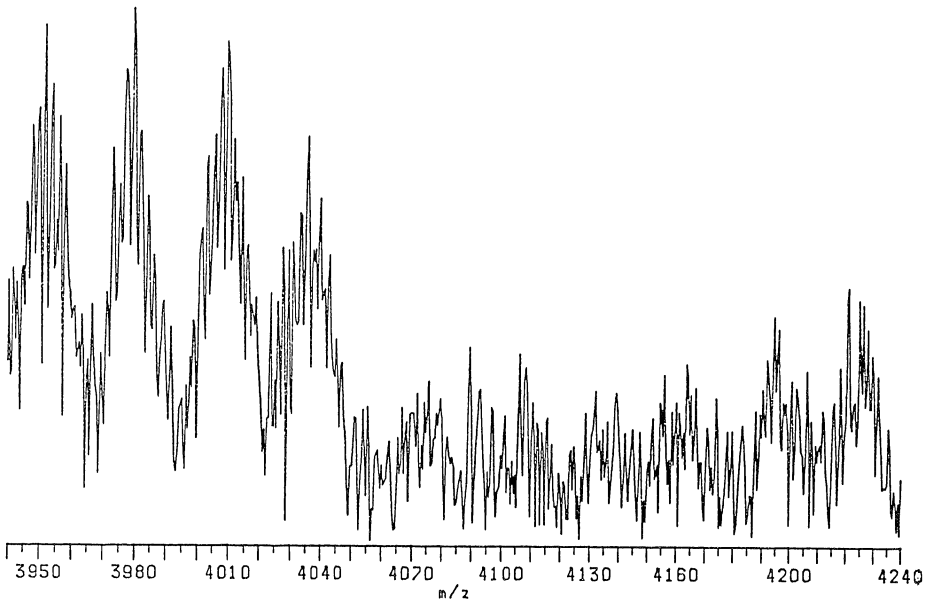

Figure 2a. Negative rheniumcarbonyl clusters with unit resolution above 4,200 amu ($2x10^{-8}$ mbar, 65 eV EI, CID activation, 1,000 scans).

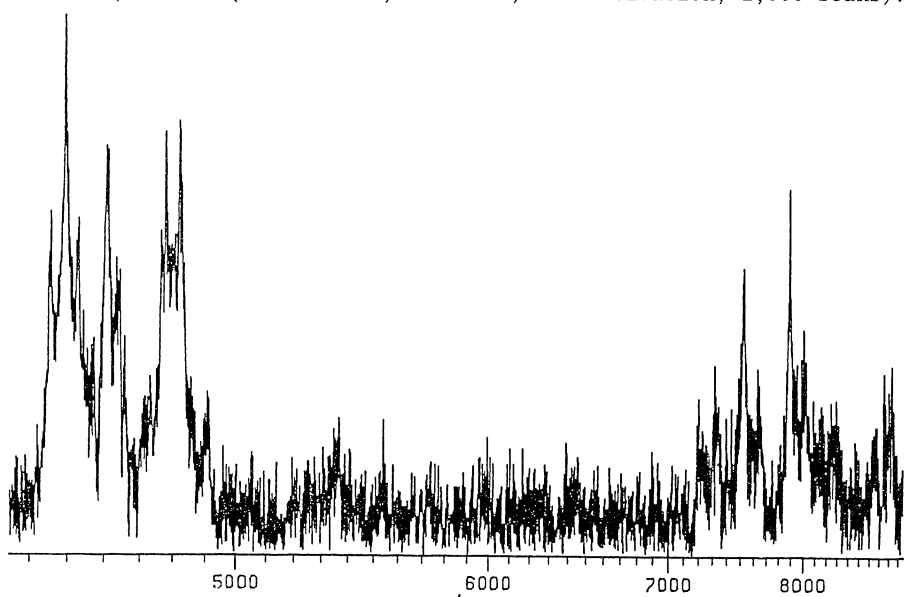

Figure 2b. Positive rheniumcarbonyl clusters with highest mass peaks > 8,800 amu ($2x10^{-8}$ mbar, 5000 scans).

The advantages of differential ion acceleration and detection in terms of rf power and signal homogeneity have been elucidated by Dunbar (4). In our cell design, rf voltages of up to 400 Volt (peak-to-peak) can be applied differentially, which allows for rapid acceleration and ejection.

Pulsed-Valve CI and CID-Experiments. Chemical Ionization (CI), self-CI (SCI), and direct or desorption CI (DCI) experiments in FTMS can be done equally well with the differentially-pumped external ion source described below, or with a pulsed-valve single cell arrangement (5,6). In our experiments, we admit a pulse of reagent gas via a piezoelectric pulsed valve with a minimum opening time of about 2.5 ms (7). Unlike solenoid pulsed valves, the performance of piezoelectric pulsed valves is not disturbed by the strong magnetic field of 4.7 Tesla.

Immediately following this pulse of reagent gas, the pressure in the ICR cell temporarily climbs to between 10^{-5} to 10^{-6} mbar. During a time delay of 1 - 2 seconds before acceleration and detection, the ICR cell is pumped down to 2×10^{-8} mbar by a 330 l/s turbomolecular pump, permitting enhanced resolution, and accurate mass determinations without internal calibrants.

Examples of both, pulsed-valve positive ion CI, using methane and ammonia as reagent ions, and pulsed-valve negative ion CI, using a N_2O/CH_4 mixture, are shown in Figure 3 a,b. In both examples the molecular ion was not stable with respect to electron impact at 70 eV, but the CI spectra clearly show abundant quasi-molecular-ion peaks.

Piezoelectric pulsed-valve inlet systems are equally useful in collision-induced dissociation (CID) experiments (8) where the CID target gas (usually Argon) is pulsed, and subsequently pumped away to permit high-resolution, high-accuracy acquisition of FTMS spectra.

Recently, low pressure CI and SCI experiments, which take advantage of the long reaction times (typically 10 to 60 seconds) possible in an FTMS, have been demonstrated (9). Figure 4 exhibits low-pressure EI and DCI spectra of Riboflavin (Vitamin B2), taken without a pulsed valve. Only the DCI spectrum taken at 2×10^{-8} mbar contains the quasi-molecular ion at M = 377.

SIMS. Secondary Ion Mass Spectrometry is particularly suited for ionization of nonvolatile, polar, and thermally labile molecules. Liquid SIMS, using liquid glycerol matrices, is best done in the differentially-pumped external ion source, because matrix effects and the high vapor pressure of glycerol make liquid SIMS unsuitable for single cell low-pressure FTMS.

Static SIMS, however, which does not require any matrix, and demands only low primary beam intensities, does not deteriorate the ultra-high vacuum in the FTMS single cell. An example of a static SIMS spectrum of Valinomycin using primary 2-4 kV Cs^+-ions is shown in Figure 5, including a high-resolution spectrum of the quasi-molecular (M+Na)-peak at mass 1133.6 amu.

In typical static SIMS experiments 1 μl of sample solution (concentration about 10^{-3} mol/l) is deposited on an etched silver surface and dried. After insertion of the silver target into the combined EI/SIMS cell via the solid sample inlet, the target is bombarded by Cs^+ for 0.02 - 10 msec with an intensity of 1-10 nanoAmp. Nearly all ions created by static SIMS are trapped at an ambient pressure of 1 - 5 x 10^{-9} mbar.

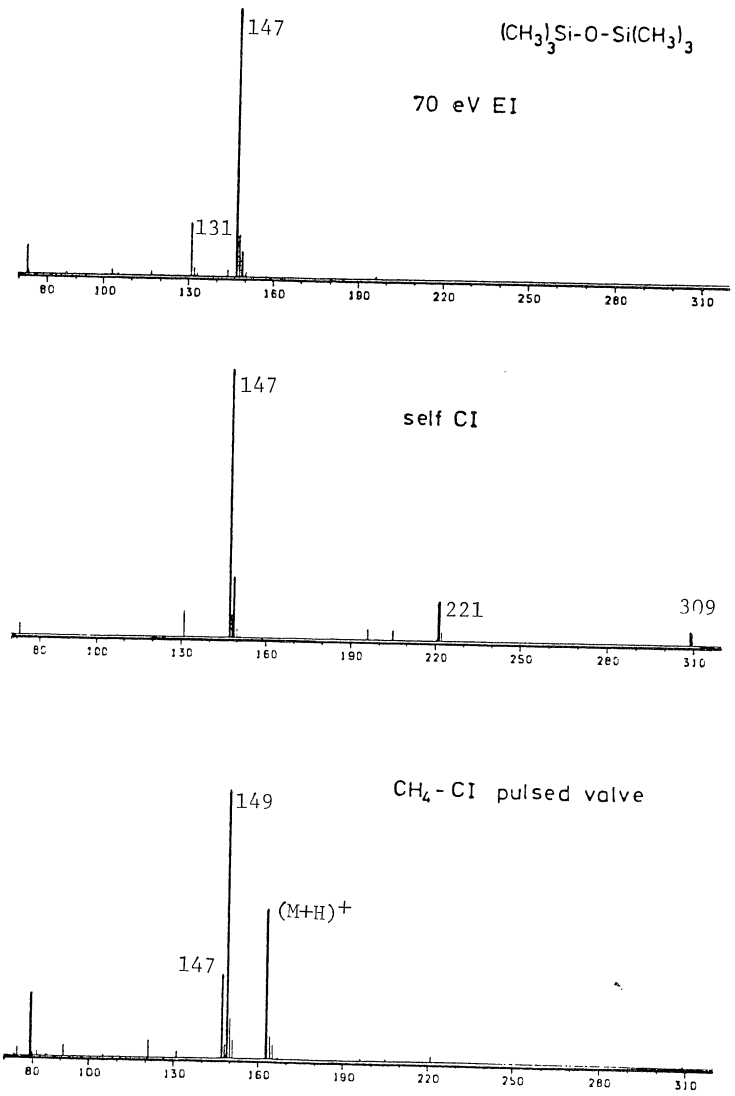

Figure 3a. 70 eV EI spectrum, self-CI, and pulsed-valve CH_4 CI positive ion spectrum of hexamethyldisiloxane.

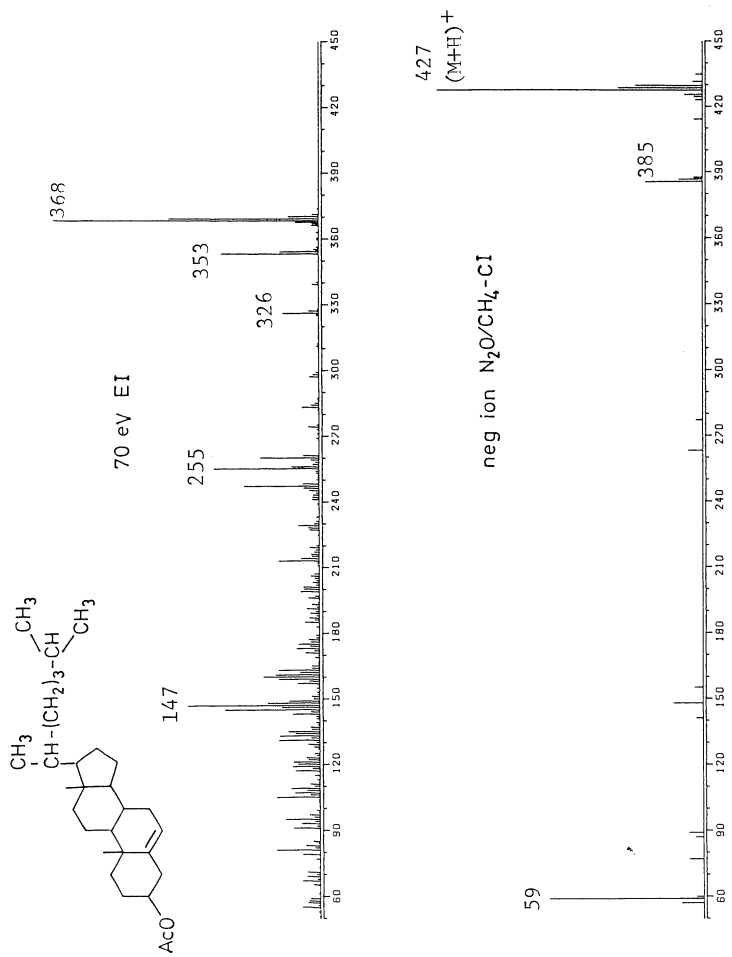

Figure 3b. 70 eV EI and pulsed-valve negative ion N_2O/CH_4-CI FTMS spectrum of cholesteryl acetate.

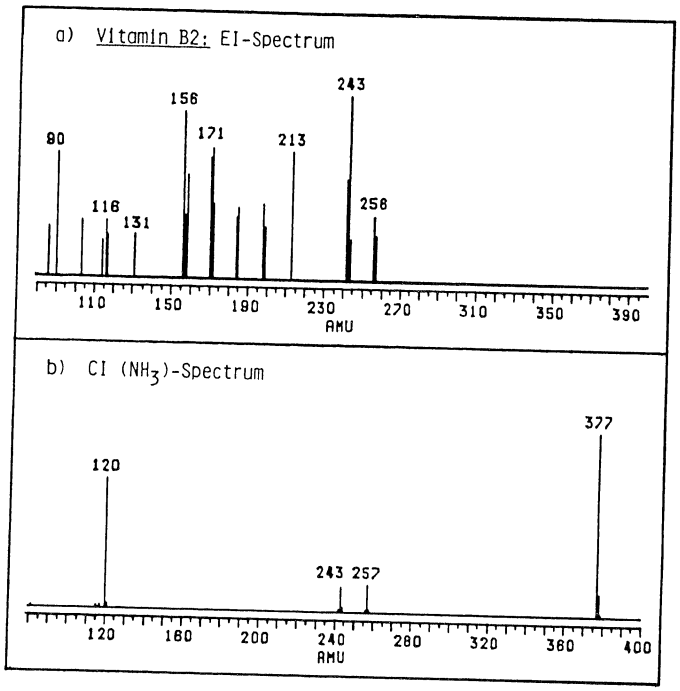

Figure 4. Low-pressure EI and DCI FTMS spectra of Riboflavin (Vitamin B2). Direct probe inlet, about 210°C.

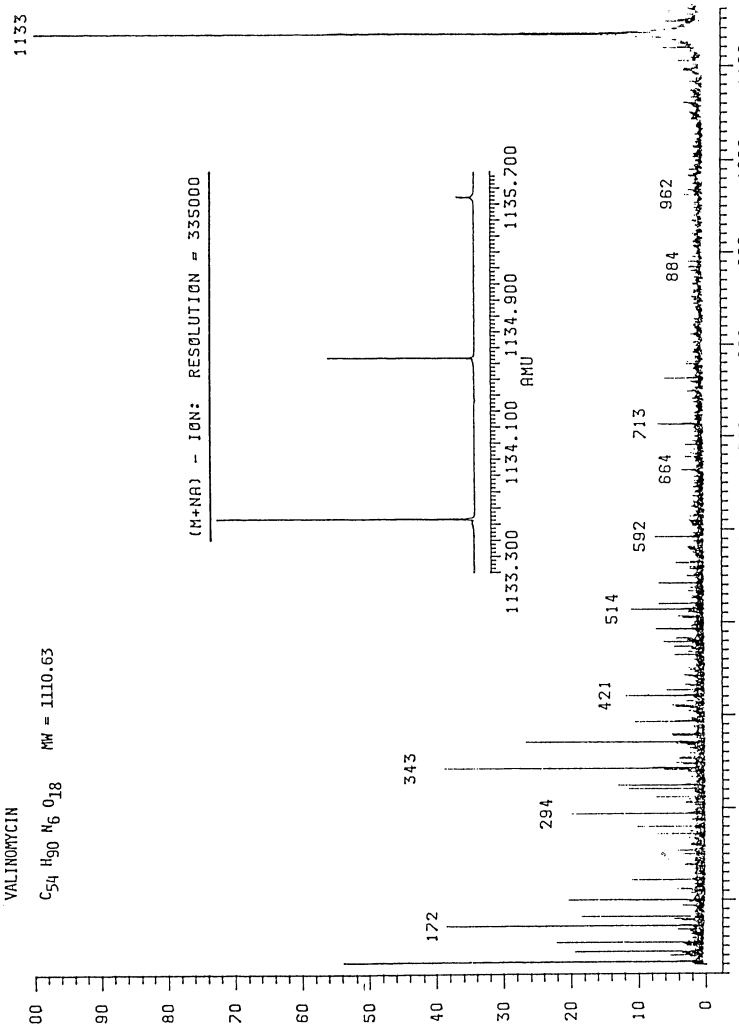

Figure 5. Static SIMS FTMS spectrum of Valinomycin, including high-resolution measurement of $(M+Na)^+$ ion with $m/\Delta m_{50\%} = 335,000$.

Magnet Requirements for FTMS

In this section the importance of both the magnetic field strength B and of the magnetic field homogeneity will be discussed. Even though analytical FTMS experiments can be done in resistive, low-field magnets, we shall restrict our discussion to superconducting magnets, which permit superior mass resolving powers and absolute mass accuracies.

Using a horizontal 4.7 Tesla cryoshimmed supercon magnet with a bore diameter of 15 cm, we have obtained two-parameter mass calibrations with absolute mass accuracies of better than 1.5 ppm without, and better than 0.4 ppm with an internal calibrant over a mass range from 18 to 502 amu (10). Absolute accuracies with an internal calibrant are slightly better because the calibrant and the unknown compound are measured under identical physical conditions, in particular with the exact same number of ions in the cell, resulting in identical space-charge shifts (2).

Due to the extreme stability of supercon magnets and the associated electronics, 2-3 ppm accuracies can be reproduced in the absence of reference compounds for many days.

Field Strength. All other conditions being equal, the mass resolving power increases linearly with field strength according to (11)

$$m/\Delta m = qB\tau/m \qquad (2),$$

where τ is the effective signal-decay time. If the linewidth is dominated by pressure broadening, as is typically the case for pressures above 10^{-9} mbar, particularly for higher masses over M = 100, then the resolution indeed improves linearly with B. In the collisional-broadening regime it is possible either to reduce the pressure or to increase the field strength in order to improve resolution.

The signal-to-noise ratio, S/N, in FTMS is given by (12)

$$S/N = \frac{Nq^2\rho B\sqrt{R}}{2md_x\sqrt{2kT\Delta f}} \qquad (3),$$

if amplifier noise is neglected. Here N is the total number of ions, ρ is the cyclotron radius, R is the resistance, T is temperature, and Δf is the detection bandwidth. Clearly, higher field strength increases the FTMS sensitivity linearly. Nevertheless, the increase of S/N with B is not as dramatic as in NMR, where sensitivity increases with the seven-fourth power of the field strength (13).

If one is interested in high-mass FTMS it is advantageous to work at the highest possible field strength, because the higher the cyclotron frequency of a given mass, the less noise is introduced during signal preamplification. Moreover, the gain of most rf power amplifiers used for acceleration, as well as the gain of the signal amplification circuitry, tend to fall off for lower frequencies, i.e. higher masses.

Finally, Equation 1 exhibits another important advantage of high fields in FTMS. Both the maximum trapping time and the maximum number of collisions (and gas-phase reactions) increase quadratically with B. Consequently increased magnetic field strength offers experimental access to larger ion clusters (Figure 2).

Homogeneity. Residual spatial magnetic field inhomogeneities limit the maximum mass resolving power to a pressure-independent upper limit, despite the fact that certain inhomogeneities are averaged by the ion motion in the cell (14). The experimental and theoretical limit of $m/\Delta m$ in our 4.7 Tesla cryoshimmed supercon magnet is approximately 10^8, as shown in Figure 6, where positive methane ions were measured with a mass resolving power of 2×10^8. In superconducting magnets without cryoshims this limit is likely to be one order of magnitude lower, and in electromagnets the upper resolution limit is about 10^5. Theoretical calculations (14) show that the maximum mass resolving power can increase by a factor between 20 and 100 to 10^9 - 10^{10}, if room-temperature shims are used in addition to the standard cryoshims.

Software Requirements for FTMS

Starting from the general philosophy that an FTICR mass spectrometer is a research grade analytical instrument, we have chosen to develop a software system which offers versatility and direct control over almost all experimental parameters.

Phasing. In order to take full advantage of FTICR's high-resolution capabilities, automatic and manual phasing have been implemented from the beginning. Consequently, in the high-resolution mode absorption spectra which require phasing can be obtained instead of magnitude spectra. Marshall (15) has pointed out that absorption spectra are narrower than magnitude spectra by a factor of $\sqrt{3}$. An example of automatic zeroth-order, and interactive first- and second-order phasing of an absorption mode spectrum is given in Figure 7, and a typical absorption mode high-resolution spectrum at mass M = 131 is shown in Figure 8. The phasing problem in broadband FTMS has not yet been solved, and usually only magnitude spectra are displayed.

Rapid Scan/Correlation ICR. In order to provide additional experimental flexibility, the CMS 47 can be operated in the rapid scan/cross correlation mode (16,17) without any hardware modifications. In this mode the receiver plates of the ICR cell are incorporated in an rf capacitance bridge circuit which detects energy absorption of the ions during a low-power rapid frequency scan using sweep rates of approximately 1 MHz/s. Rapid scan/correlation ICR can be utilized advantageously when very large mass ranges are to be detected, and particularly when large mass ranges extend into the low mass/high frequency region below mass M = 20. An example of a cross correlation spectrum is given in Figure 9. With standard FT-NMR phasing techniques both absorption and magnitude spectra can be obtained (16). Rapid scan/cross correlation ICR has the additional advantage that intensity ratios are reproduced more accurately than in FTICR.

Versatile Pulse Sequence. One of the great strengths of FTMS is the flexibility to selectively accelerate, activate, and eject ions in any combination and any sequence without hardware modifications. This versatility makes FTMS the method of choice for MS/MS and hence for establishing pathways and rate constants for gas-phase ion-molecule reactions, and to correlate this data with structural information. Recently up to $(MS)^5$ has been demonstrated (18).

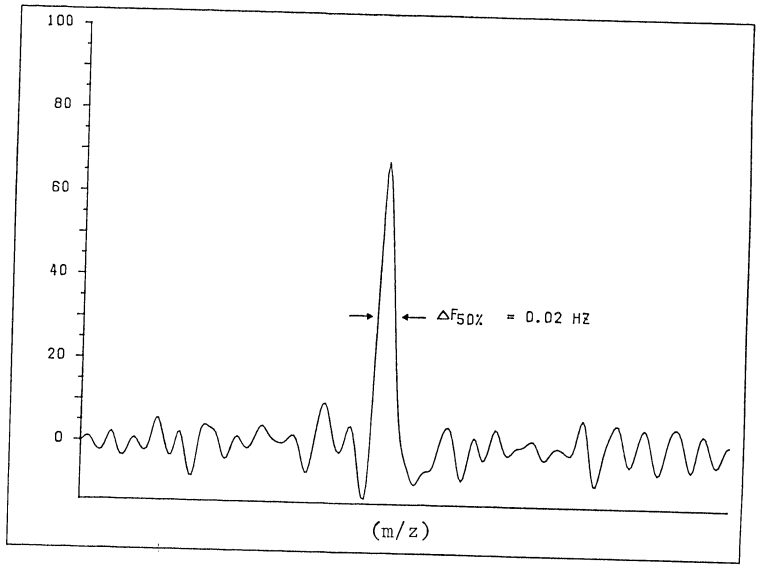

Figure 6. Ultra-high resolution FTMS spectrum of positive methane ions with $m/\Delta m_{50\%} = 2 \times 10^8$, $\Delta f_{50\%} = 0.02$ Hz.

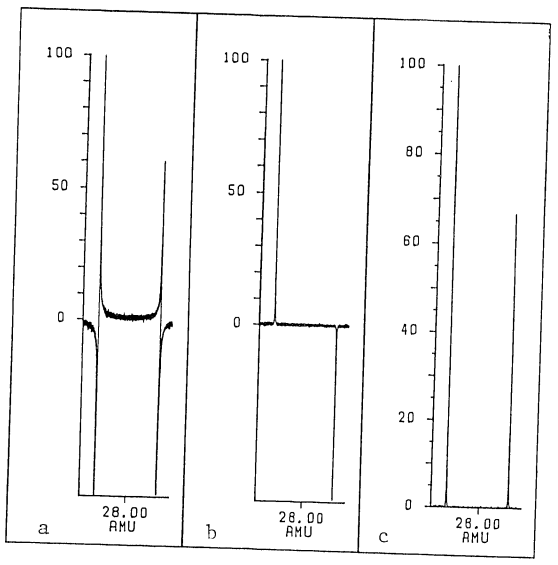

Figure 7. High-resolution absorption mode peaks of N_2^+ and CO^+: a) unphased, b) after automatic zeroth-order phasing, c) after interactive first- and second-order phasing.

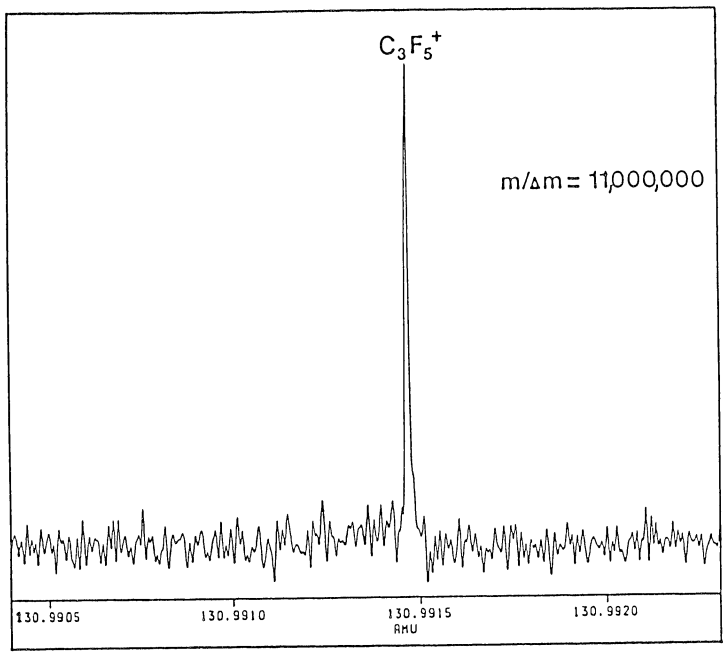

Figure 8. High-resolution absorption mode spectrum of C_3F_5+ at mass 131 amu. Resolution $m/\Delta m_{50\%}$ = 11,000,000.

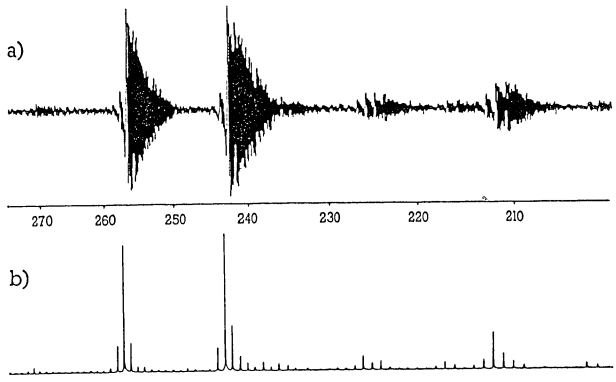

Figure 9. a) Rapid scan spectrum b) cross correlation spectrum.

To exploit the advantages of FTMS fully we have implemented several predefined ejection, activation and acceleration options, like single shots, covers, sweeps over some mass window, sweeps around some unaccelerated mass window, tickling belts with phase inversion, parent ion selection chirps, activation shots for daughter ion production, etc.

Using automation software routines for the ASPECT 3000 pulse generator, we can utilize up to nine ejection/activation pulses, each combining up to four options. Mass (or frequency) information is taken from several variable user-defined lists, such that each option in each event may be used on a large number of masses. The variable mass and delay lists can be defined either via alphanumeric keyboard input, or they can be defined interactively from the spectrum via cursor. Each acceleration/ejection event can contain up to 4095 different steps. All events can be separated by fixed or incrementable delays.

Computer Interpretation, Timesharing and Throughput. For routine applications and high throughput, timesharing is essential. On the CMS 47 three so-called jobs can run in timesharing mode. For instance, job 1 may be acquiring data, job 2 may plot previously taken data, while the user is defining the parameters of the next experiment in job 3 in a menu-driven fashion.

Finally, for routine applications, our software provides a database management system called BASIS for storage and manipulation of chemical information. BASIS can access generally available spectral libraries from three different spectroscopic techniques (MS, H-NMR and $F^{1}3C$-NMR, IR), and permits the creation of new libraries. For structure elucidation and substructure search of unknown compounds, library search algorithms allow the retrieval of identical and structurally similar spectra.

External Ionization

Typical pressures in the analyzer region of FTICR mass spectrometers are about three orders of magnitude lower than in most other types of mass spectrometers. For instance in our single cell CMS 47 we can routinely obtain pressures of $3x10^{-10}$ mbar using a 330 l/sec Balzers turbomolecular pump. It is very difficult to couple existing, high gas-load GC-MS, LC-MS, liquid SIMS, or FAB ion sources directly into a single-cell configuration. Other ionization techniques like static SIMS and Laser Desorption (LD) can be operated with much improved throughput in a medium-pressure source.

It is therefore evident that a differentially-pumped ion source, operating at 10^{-5} to 10^{-6} mbar, is a desirable feature of an FTICR mass spectrometer, particularly for routine applications. Three approaches are presently followed to implement differentially-pumped ion sources: the dual cell which is described elsewhere in this book, and external ionization with (19) and without (20) tandem quadrupoles.

External ionization has the advantage of completely removing the ionization region from the narrow magnet bore while retaining all the features which make FTMS such an attractive technique, like high resolution, accurate mass determinations, wide mass range, long trapping times, selective ejection/activation/acceleration etc. Our external ion source, which uses simple accelerating and focusing elements, greatly improves access to the ionizer, thereby facilitating the coupling of various inlet systems, without the need

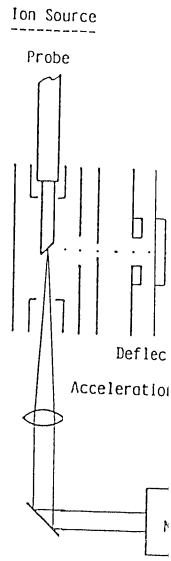

Figure 10. differentially p

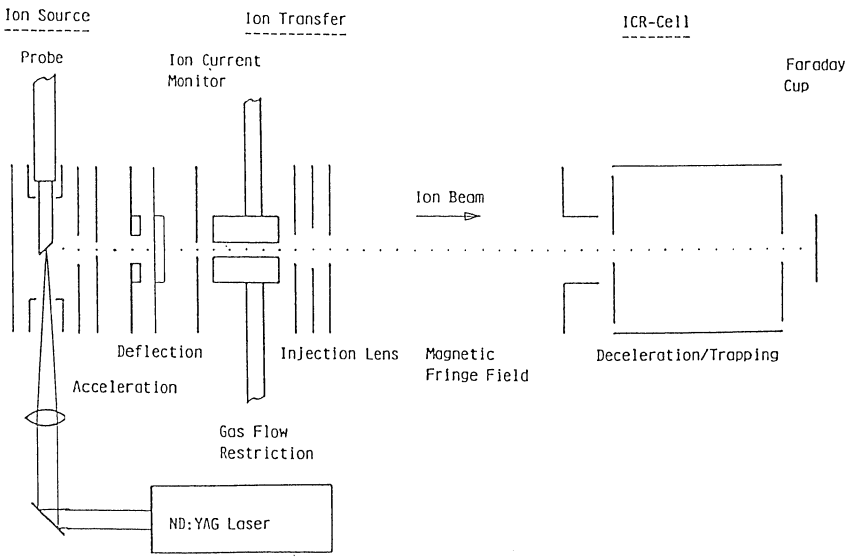

Figure 10. Schematics of ion transfer mechanism from differentially pumped external ion source with LD.

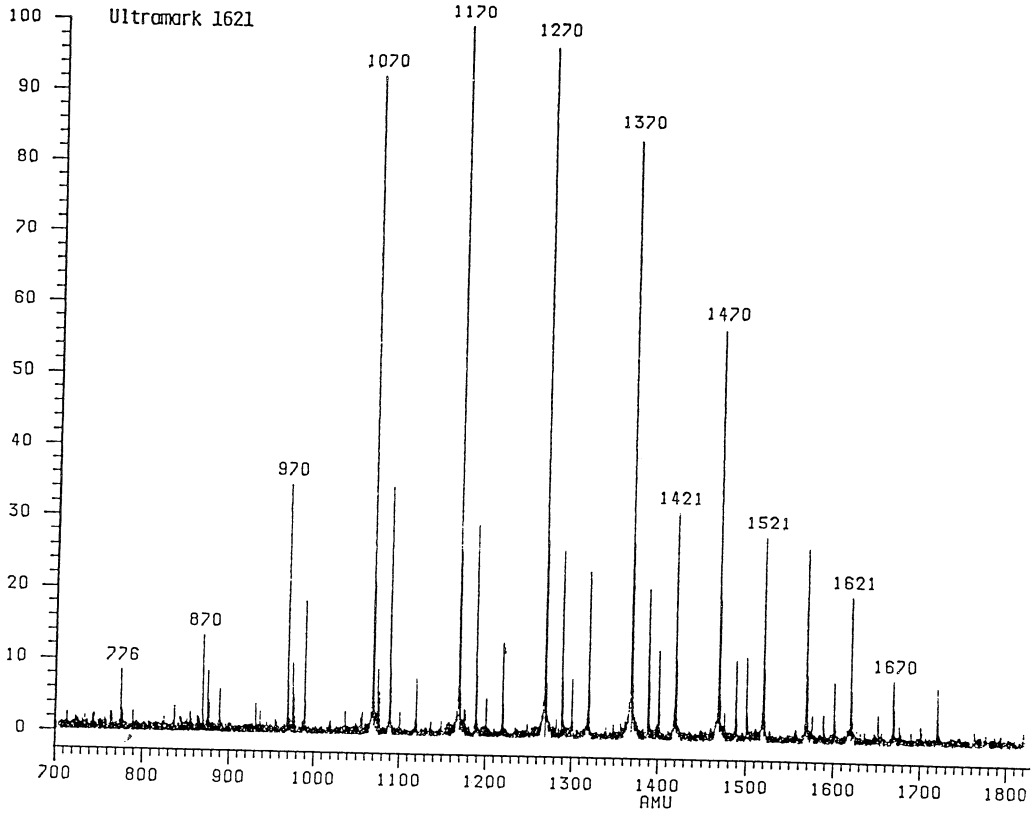

Figure 11a. Positive ions of Ultramark 1621. Electron impact ionization with direct insertion probe in external ion source.

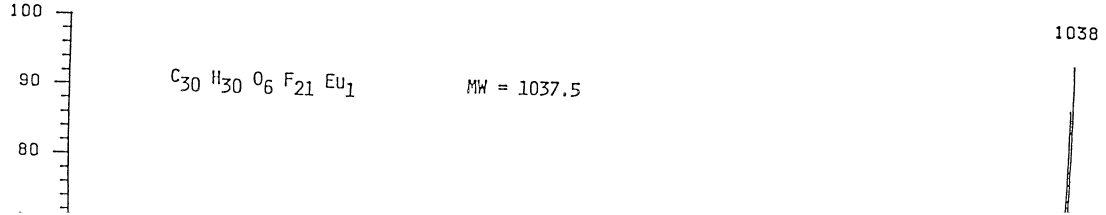

Figure 11a. Positive ions of Ultramark 1621. Electron impact ionization with direct insertion probe in external ion source.

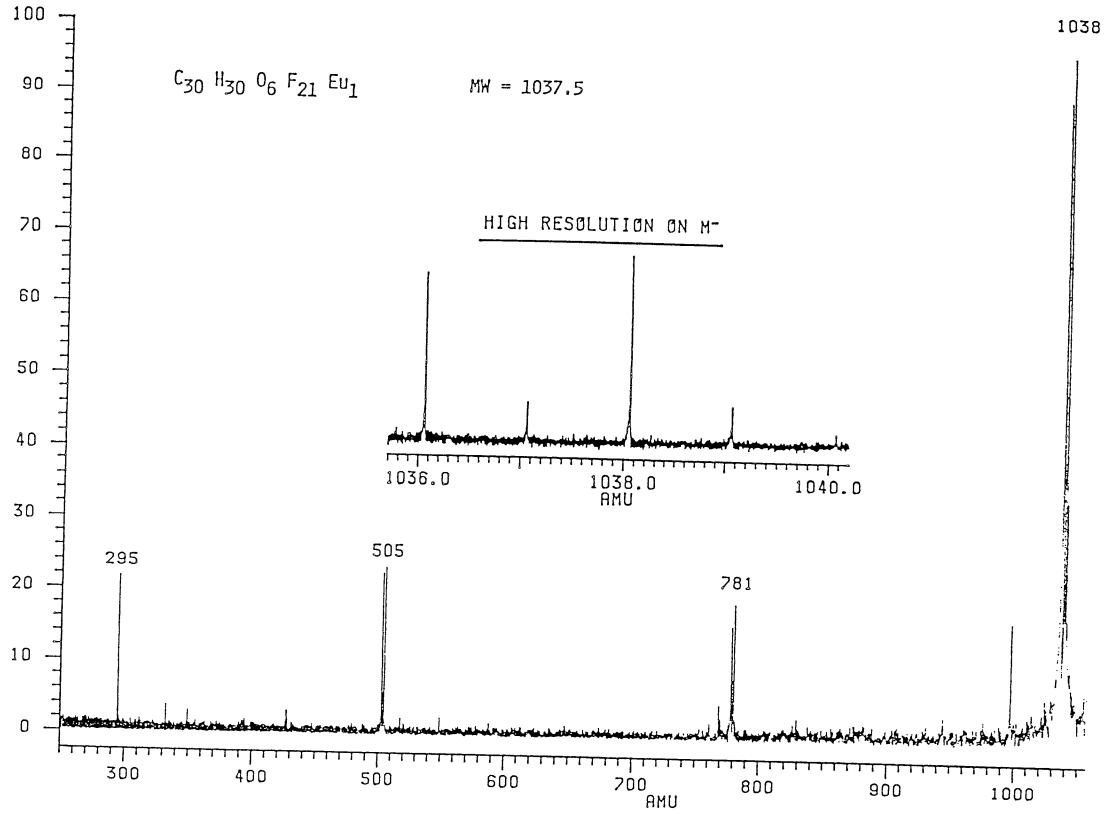

Figure 11b. Negative ions of Euroshift-FOD. Laser desorption in external ion source using a Spectron Nd:YAG laser focused to about 10^9 W/cm^2 for 8 nsec.

for expensive and experimentally more complex rf quadrupoles. It does not provide for mass preseparation outside the magnet, but mass selection can be obtained with FTMS double resonance techniques. Typical ion current transmission efficiencies are of the order of 30%. The ion transfer efficiency from source to analyzer is mass-independent (20). For special analytical applications, time-of-flight effects during ion transmission can be utilized to separate certain mass windows by setting appropriate time intervals between EI or LD ionization and the cell trapping pulse (21).

Figure 10 shows a schematic drawing of the ion transfer mechanism in the CMS 47 with external ionization. Figure 11a presents the mass spectrum of Ultramark 1621 using electron impact in the external source, and Figure 11b depicts a broadband spectrum and the high-resolution window of the negatively charged molecular ion of Euroshift-FOD after laser desorption in the external ion source. Moreover, the external ion source can be employed for medium-pressure CI and SCI as an alternative to the low-pressure and pulsed-valve CI techniques described above.

Anticipated Developments in FTMS Instrumentation

With the successful implementation of differentially-pumped external ion sources, FTMS is rapidly becoming a routine mass spectrometric technique. Medium-pressure interfaces for the coupling of GC, LC, FAB, and liquid SIMS into the external ionizer are currently under development, and should become available in the near future.

Recently, new 2D-methods for the analysis of complex mixtures have been developed for time-of-flight mass spectrometry (22), which could also be utilized in external ionization FTMS. Specifically, the combination of IR-laser desorption of nonvolatile neutrals, followed by adiabatic cooling to 2°K in a supersonic jet, and subsequent compound-selective Resonance-Enhanced Multiphoton Ionization (REMPI) could increase the role of FTMS in the analysis of biological mixtures. The coupling of supersonic jets to the external ion source would also be of interest in ion- and neutral cluster experiments.

Finally, it is conceivable that ultra-high resolution FTICR will find additional applications in particle, nuclear, and atomic and molecular physics. We believe that some of the instrumental prerequisites for these applications will include a) working at lower pressures below 10^{-11} mbar, b) better magnetic field homogeneity using additional room-temperature shims and employing improved shimming techniques (14), and c) ultra low-noise preamplifiers capable of detecting single or very few ions.

Acknowledgments

FHL wishes to thank Professor William Klemperer at Harvard University for his encouragement and guidance. The authors thank Robert A. Forbes for his suggestions and for reading the manuscript. Finally the authors are grateful to Michelle V. Buchanan for her tremendous efforts in organizing this FTMS book.

Literature Cited

1. Wanczek, K.P. Int.J. Mass Spectrom. Ion Processes 1984, 60, 11-60.

2. Jeffries, J.B.; Barlow, S.E.; Dunn, G.H. Int.J. Mass Spectrom. Ion Processes 1983, 54, 169.
3. Francl, T.J.; Fukuda, E.K.; McIver, R.T. Int.J. Mass Spectrom. Ion Physics 1983, 50, 151.
4. Dunbar, R.C. Int.J. Mass Spectrom. Ion Processes 1984, 56, 1.
5. McIver, R.T. 30th An. Conf. Mass Spectrom. All. Top. A.S.M.S., Honolulu 1982.
6. Freiser, B.S. 30th An. Conf. Mass Spectrom. All. Top. A.S.M.S., Honolulu 1982.
7. Zwinselman, J.J.; Allemann, M.; Kellerhals, Hp. Spectrospin ICR Application Note 1984, IV.
8. Cody, R.B.; Freiser, B.S. Anal. Chem. 1982, 54, 1431.
9. Grossmann, P.; Allemann, M.; Kellerhals, Hp. Spectrospin ICR Application Note 1986, VI.
10. Klass, G.; Allemann, A.; Bischofberger, P.; Kellerhals, Hp. Spectrospin ICR Application Note 1983, II.
11. Marshall, A.G.; Comisarow, M.B.; Parisod, G. J. Chem. Phys. 1979, 71 (11), 4434.
12. Comisarow, M.B. J. Chem. Phys. 1978, 69 (9), 4097.
13. Hoult,D.I.; Richards,R.E. J. of Magn. Reson. 1976, 24, 71.
14. Laukien,F.H. Int.J. Mass Spectrom. Ion Processes 1986, 73, 81.
15. Marshall,A.G. In Fourier, Hadamard and Hilbert Transforms in Chemistry; Marshall,A.G.,Ed.; Plenum Press: New York, 1982; Chapter 1.
16. Parisod,G.; Gaumann,T. Chimia 1980, 34, 271.
17. McIver,R.T.; Hunter,R.L.; Ledford,E.B.; Locke,M.J.; Francl,T.J. Int. J. Mass Spectrom. Ion Phys. 1981, 39, 65.
18. Forbes,R.A.; Laukien,F.H.; Wronka,J. submitted to Int.J. Mass Spectrom. Ion Processes.
19. Hunt,D.F.; Shabanowitz,J.; Yates,J.R.; McIver,R.T.; Hunter,R.L.; Syka,J.E.P.; Amy,J. Anal. Chem. 1985, 57, 2728.
20. Kofel,P.; Allemann,M.; Kellerhals,Hp. Int.J. Mass Spectrom. Ion Processes 1985, 65, 97.
21. Kofel,P.; Allemann,M.; Kellerhals,Hp. Int.J. Mass Spectrom. Ion Processes 1986, 72, 53.
22. Frey,R. 34th An. Conf. Mass Spectrom. All. Top. A.S.M.S., Cincinnati, 1986.

RECEIVED June 15, 1987